Minireview

Structure, dynamics and function of the outer membrane protein A (OmpA) and influenza hemagglutinin fusion domain in detergent micelles by solution NMR

Lukas K. Tamm[a,*], Frits Abildgaard[b], Ashish Arora[c], Heike Blad[b], John H. Bushweller[a]

[a] *Department of Molecular Physiology and Biological Physics, University of Virginia, Charlottesville, VA 22908-0736, USA*
[b] *NMRFAM, University of Wisconsin, Madison, WI 53706, USA*
[c] *Molecular and Structural Biology, Central Drug Research Institute, Lucknow 226 001, UP, India*

Received 25 August 2003; accepted 1 September 2003

First published online 7 October 2003

Edited by Gunnar von Heijne, Jan Rydström and Peter Brzezinski

Abstract Recent progress from our laboratories to determine structures of small membrane proteins (up to 20 kDa) in detergent micelles by solution nuclear magnetic resonance (NMR) is reviewed. NMR opens a new window to also study, for the first time, the dynamics of membrane proteins. We report on recent attempts to correlate dynamic measurements on OmpA with the ion channel function of this protein. We also summarize how NMR and spin-label electron paramagnetic resonance spectroscopy and selective mutagenesis can be combined to provide a structural basis towards understanding the mechanism of influenza hemagglutinin-mediated membrane fusion.

Key words: Nuclear magnetic resonance; Membrane protein; OmpA; Influenza hemagglutinin; Structure–function relation; Dynamics

1. Introduction

Membrane proteins are the 'last frontier' of structural biology. Despite their prominence in the genomes of all organisms and their importance as drug targets, progress in determining their structures has been much slower compared to the breathtaking progress in structure determination of soluble proteins in the era of structural genomics. However, even this is changing; 2003 promises to become a particularly fruitful year for the structural biology of membrane proteins. Many new high resolution membrane protein structures have been solved by all three principal structural techniques, i.e. X-ray crystallography, electron microscopy, and nuclear magnetic resonance (NMR). Solid-state NMR has long been proposed as the preferred NMR technique to study membrane proteins [1]. However, with the recent advent of ever higher magnetic fields and transverse relaxation optimized spectroscopy (TROSY) [2], small (~20 kDa) membrane proteins in detergent micelles can be solved by solution NMR techniques. Here, we summarize some of our own experience using solution NMR to study structure–function relationships of the OmpA transmembrane (TM) domain and the membrane-embedded fusion domain of influenza hemagglutinin.

2. OmpA transmembrane domain

OmpA is an abundant structural protein of the outer membrane of Gram-negative bacteria [3]. It is believed to connect the outer membrane structurally to the periplasmic peptidoglycan layer via its periplasmic domain, which consists of residues ~177–325. Residues 1–~172 form the TM domain, whose structure has been solved by X-ray crystallography [4] and NMR [5]. As had been predicted before from its sequence [6] and refolding studies [7], the TM domain of OmpA forms an eight-stranded β-barrel in detergent micelles and lipid bilayers. When reconstituted into planar lipid bilayers, OmpA forms an ion channel [8,9], which may be slightly anion-selective (R. Wagner and L. Tamm, unpublished results). Although full-length OmpA exhibits two different types of single channel conductance steps, the TM domain alone only produces the smaller channels (60–70 pS, in 0.1 M KCl). Other functions that have been attributed to OmpA are its involvement in bacterial conjugation [10] and its action as receptor for various bacteriophages [11,12] and some colicins [13].

The exploration of conditions to over-express and spontaneously refold OmpA into detergent micelles [14,15] and lipid bilayers [7,16,17] has greatly facilitated its structure determination by NMR [5]. Refolded OmpA exhibits similar single channel properties as native OmpA [9]. For NMR studies, the signal sequence was removed, the protein was over-expressed in *Escherichia coli*, and purified in a urea-denatured form from inclusion bodies. The protein was refolded into dodecylphosphocholine (DPC) micelles and TROSY-based NMR spectra were recorded at 600 and 750 MHz proton frequency. The size of the detergent/protein complex was ~46 kDa, based on dynamic light scattering measurements. The expressed TM domain comprising residues 1–177 has a calculated molecular weight of 19 175 Da. Therefore, about 60% of the complex is detergent, amounting to about 76 molecules of DPC per complex. DPC alone forms micelles of 70–80 molecules above the critical micelle concentration of 1.5 mM. Best spectra were obtained in a large excess of detergent (600:1

*Corresponding author. Fax: (1)-434-982 1616.
E-mail address: lkt2e@virginia.edu (L.K. Tamm).

0014-5793/03/$22.00
doi:10.1016/S0014-5793(03)01127-X

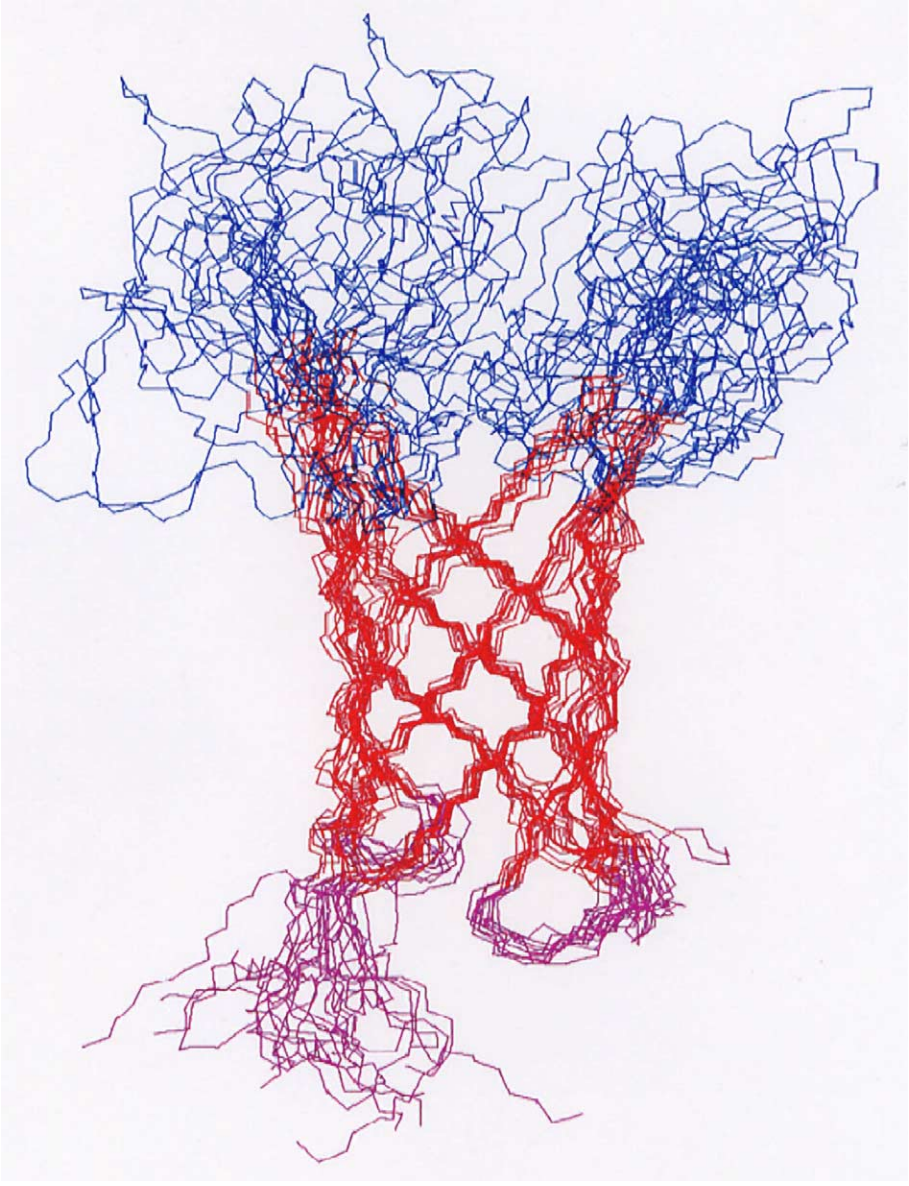

Fig. 1. Ten lowest energy structures of the OmpA transmembrane domain in DPC micelles determined by heteronuclear solution NMR (from [5]).

DPC:protein), which implies that ~85% of the micelles did not contain protein.

Residues of triple-labeled (^{15}N, ^{13}C, ^{2}H) protein were assigned using four different three-dimensional heteronuclear NMR experiments. Since a minority conformation appeared to exist even under large excess detergent conditions, it was necessary to prepare several specific amino acid-labeled samples to aid the assignment process. Eventually, 156 (88%) of the 177 residues could be assigned. The unassigned residues were all in the unstructured N- and C-terminal tails or in the three extracellular loops that exhibited unusually large dynamic mobilities (see below). The backbone fold of the OmpA TM domain was initially calculated from 91 nuclear Overhauser effect (NOE) distance constraints and 142 torsional angle constraints. The eight-stranded β-barrel of the OmpA TM domain was clearly defined by these NMR measurements. The structure was subsequently refined by introducing 116 hydrogen bond constraints between adjacent β-strands that had been identified in the initial fold calculations (Fig. 1). The strands of the barrel are connected by three tight turns on the periplasmic side and four large loops on the extracellular side. The structure of the barrel is well-defined (rmsd of backbone atoms = 1.19), but that of the loops is not. The lack of well-defined structures of the loops is not only the result of a lack of assignments in this region, but reflects an intrinsic high mobility of these loops in the structure of OmpA, as directly demonstrated by NMR measurements of the backbone dynamics.

In order to obtain direct insight into the backbone dynamics of the OmpA TM domain, we measured ^{15}N transverse and longitudinal relaxation times and $\{^{1}H\}$-^{15}N heteronuclear NOEs at 500, 600, and 750 MHz proton frequency. Relaxation data in proteins are often analyzed in terms of the 'model-free approach', where the local and global motions are thought to be independent of one another [18,19]. We analyzed our results in terms of an extended Lipari–Szabo model

(manuscript in preparation). In our implementation, unbiased motional parameters were extracted in an improved analysis that (a) takes into account anisotropic tumbling of the detergent/protein complexes in solution [20], (b) allows for simultaneous individual and segmental motions on two time scales (ps and ns), and (c) includes conformational exchange on the μs–ms time scale as a contributing factor to the measured relaxation data. To achieve this goal, the nine data sets were simultaneously globally fit to this extended model (manuscript in preparation).

The diffusion tensor emerging from the global fit was quite anisotropic. Rotation around the z-axis, which was approximately co-linear with the barrel axis, was 1.8 times faster than rotation around the other axes. The ratio of the two perpendicular diffusional correlation times was 1.3. Although all assigned residues exhibited motions in the 10–200 ps range, some residues in addition also displayed motions in the 1–3 ns range. The time scale of these slow internal motions was distinct from that of the overall rotational correlation time of the protein/detergent micelle, which was ~20 ns. Most ns motions were found in the four extended loops indicating that these might undergo large concerted motions on the ns time scale. Periplasmic turn number 2, but not turns number 1 and 3, also displayed large-amplitude ns motions. All strand residues, with the exception of a very few at the strand/loop boundary, lacked ns motions. Their ps motions were also more restricted, i.e. their order parameters, S^2, were larger than those of the loops.

A few residues of the barrel exhibited conformational exchange on the μs–ms time scale. These are highlighted in the structural model presented in Fig. 2. Except for strands 1 and 6, all strands have some residues that exhibit conformational exchange. Most residues that show conformational exchange are located in the mid-section of the barrel, but a few are also found at either end of the barrel. Those in the mid-section are Arg 96, Arg 138, Lys 82, and Tyr 94, which have all been shown to participate in an intricate hydrogen-bonding network in the lumen of the barrel [4]. Other residues that participate in the hydrogen-bonding network do not show conformational exchange themselves, but have nearest neighboring residues that do. E.g., Met 53 next to hydrogen-bonded Glu 52, and Val 166 and Tyr 168 next to hydrogen-bonded Ser 167 and Arg 169 all exhibit significant conformational exchange. These results strongly indicate that the hydrogen-bonded core of the OmpA TM domain is not completely rigid, but subject to motions on the μs–ms time scale.

Conformational flips of polar and charged side chains may contribute to the channel function of OmpA. Supported by molecular dynamics calculations, it was hypothesized that the channel gate is formed by a salt bridge between Arg 138 and Glu 52 [21]. Both of these residues either show conformational exchange themselves or are nearest neighbors of a residue that shows conformational exchange. In the model of Bond et al. [21], Arg 138 is thought to break its salt bridge to Glu 52, but form a new one to Glu 128 on the same channel wall when the gate is opened. However, Glu 128 does not show conformational exchange according to our NMR measurements, but Lys 82, which is near and on the same side as Glu 52, does show conformational exchange. Therefore, an alternative model for channel opening might be a conformational rotation of the Glu 52 side chain to let it form a new salt bridge with Lys 82 on the same side of the channel. The two opening mechanisms are not mutually exclusive and could happen at the same time. Even though an unambiguous mechanism for channel conductance does not yet emerge from these measurements, the example of OmpA shows that dynamics measurements by NMR may be very useful to contribute to a deeper understanding of the function of membrane channels.

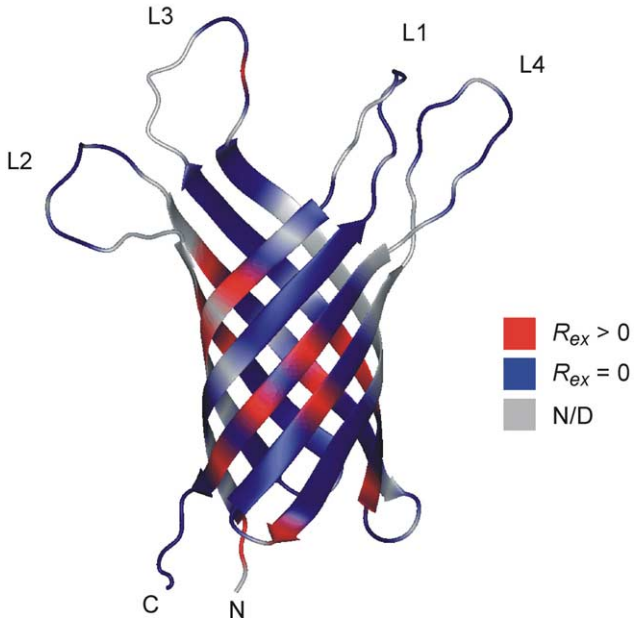

Fig. 2. Residues of the OmpA TM domain that show conformational exchange on the μs–ms timescale are mapped onto the NMR structure (unpublished results).

3. Influenza hemagglutinin fusion domain

Influenza virus enters cells by endocytosis followed by pH-triggered fusion of the viral membrane envelope with the endosomal membrane. The pH in the endosome needs to reach a value below a threshold of about pH 5.5 in order to fuse viral particles. Fusion is mediated by influenza hemagglutinin (HA), a type I integral membrane protein that is expressed on the surface of influenza virus particles. The entire molecule is a trimer of 220 kDa. Each subunit consists of an HA1 and HA2 polypeptide chain. The HA2 chain begins with a quite hydrophobic peptide, the 'fusion peptide', that is highly conserved between different strains of influenza virus and that is indispensable for membrane fusion. Even minor amino acid changes in this region cause dramatic differences in the fusion phenotypes. It has also been shown that the fusion peptide of HA is the only region of HA (besides the TM domain) that interacts strongly with and inserts deeply into cellular target membranes during fusion. Because this peptide of about 23 residues is linked to the remainder of the protein via a flexible hinge, and because the peptide appears to fold in membranes independent of the soluble ectodomain of HA, the peptide has also been termed the 'fusion domain' of HA.

We have recently solved the structure of the HA fusion domain in detergent (DPC) micelles at pH 7 and 5 by ^{1}H NMR [22]. The pH 5 structure is shown in Fig. 3. It is characterized by an N-terminal α-helix, a kink region, and a short C-terminal 3_{10}-helix. The turn forming the kink is defined by hydrogen bonds from the NHs of Glu 11 and Asn 12 to the

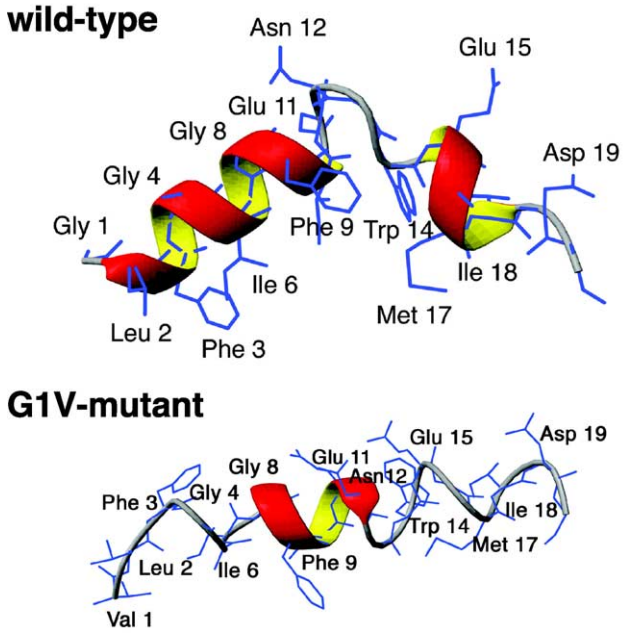

Fig. 3. NMR structures of influenza HA fusion peptides bound to DPC micelles in pH 5 buffer. The wild-type peptide at the top shows an angled amphipathic boomerang structure. The G1V mutant below forms a linear and less regular amphipathic helix. Spin-label EPR data indicate that the global features of both structures are retained, when bound to membranes, and that they penetrate quite deeply into one leaflet of the lipid bilayer (see text; wild-type from [22]).

carbonyls of Gly 8 and Phe 9, respectively, and additional NH-to-carbonyl hydrogen bonds from Asn 12 to Gly 8 and Trp 14 to Phe 9, which however are observed in only 50% of the structures. This turn imposes an overall 'V' or 'boomerang' shape on the fusion peptide in detergent micelles. The outer surface of the boomerang is characterized by a consecutive stretch of glycine residues in the N-terminal arm (Gly 1, 4, and 8) and polar and charged residues in the kink and C-terminal arm. The inner surface of the boomerang is lined exclusively with apolar residues including three aromatic ones. They form a hydrophobic pocket within the angle of the structure.

Site-directed spin-label electron paramagnetic resonance (EPR) spectroscopy was used to determine whether the structure determined by NMR in micelles is retained in membranes [22]. Every single residue was individually changed to a cysteine and labeled with a small nitroxide spin label. The depths of the spin labels in lipid bilayers were determined by power saturation and their accessibility to oxygen in the membrane and a nickel complex in solution. This method allows one to determine the depth of membrane penetration of each residue with a resolution of $\sim$3 Å [23]. When applied to the fusion domain of HA, we found that the boomerang structure determined by NMR was retained in lipid bilayer model membranes to the resolution of the EPR method. Apparently, the NMR structure is not an artifact of the micelle system that had been used to obtain the high resolution structure, but represents the structure in lipid bilayer membranes. In addition, the EPR method also positions the whole peptide in the membrane. The deepest side chains, Leu 2 and Phe 3, reach as far as about the center of the lipid bilayer and the Asn 12 vertex of the boomerang is about co-planar with the phosphates of the phospholipid headgroups in the membrane [22].

Structure–function relationships may be established by site-directed mutagenesis in the fusion peptide region of full-length HA and correlating changes of fusion phenotypes with structural changes of the peptide models. Two mutations of the N-terminus are particularly interesting and instructive. When Gly 1 is changed to a serine, HA is able to induce 'hemifusion', but not full fusion. The hemi-fused state is thought to be an intermediate state, in which the lipid bilayers of the two membranes are connected, but a fusion pore has not yet been opened [24]. The overall structure of the G1S mutant peptide is still boomerang-shaped, i.e. very similar to the wild-type structure, but the glycine edge is disrupted by an unusual hydrogen-bonded N-terminal cap structure (manuscript in preparation). Conservation of the glycine edge in the N-terminal helix may thus be important at a late stage in membrane fusion, namely the transition from the hemi-fused to the fully fused state.

When Gly 1 is changed to a valine, pH-dependent fusion mediated by full-length HA is arrested altogether [24]. Not even the hemi-fused state is reached with this mutant although HA is properly expressed and the pH-induced conformational change of the ectodomain occurs as in wild-type HA. The changed phenotype must have something to do with the structure or mode of membrane insertion of the mutant fusion domain. Circular dichroism spectra of the G1V fusion domain in model membranes and micelles show that its helical content is reduced. Isothermal titration calorimetry further shows that the enthalpy and free energy of binding to lipid bilayers of G1V is also reduced compared to the wild-type protein [25]. The NMR structure of G1V in DPC micelles is dramatically different from that of the wild-type. The G1V mutant fusion domain forms a quite irregular linear helix (Fig. 3). The kink at Asn 12 is abolished in this structure. The detergent micelle interface provides a means to propagate a seemingly minor conformational change at the N-terminus all the way to the kink region. Gly 1 of the wild-type peptide points upward, away from the core of the membrane. The hydrophobic Val 1 of the mutant peptide points down towards the core of the membrane or micelle. It thereby destroys some of the strong amphipathic helical character of the N-terminal arm of the wild-type peptide to the extent that it destabilizes the kink at Asn 12. Recent unpublished spin-label EPR experiments from our laboratory indicate that the linear structure of the G1V mutant is also retained in lipid bilayers. Therefore, the structural change observed by NMR in micelles appears to be preserved in lipid bilayers. Extrapolating boldly from the results with this single mutant, one might conclude that the boomerang shape is important for initiating the first step in membrane fusion, namely to form the partial merging of the two membranes to form the hemi-fused intermediate. Similar experiments with more mutants will be needed to corroborate this 'boomerang hypothesis' of HA-mediated membrane fusion [26].

4. Prospects and conclusion

Solution NMR is becoming a viable alternative to solve the structures of membrane proteins in detergent micelles, provided these structures are not too large. The structures (back-

bone folds) of three membrane proteins have been solved by these methods [5,27,28]. They are all β-barrels in the molecular mass range of about 20 kDa. The structures of β-barrel membrane proteins are easier to solve than those of α-helical membrane proteins for two reasons. First, the ^{1}H chemical shift dispersion is larger for β-sheets than for α-helices. This difference is accentuated in membrane proteins because TM β-barrels have alternating hydrophilic/hydrophobic residues and TM α-helices have many consecutive aliphatic residues with often very similar chemical shifts. Second, β-barrels are thermally sturdier than α-helical bundle membrane proteins. Some helical membrane proteins cannot be exposed to higher temperatures for extended periods of time without loss of activity, which sometimes is necessary to obtain well-resolved NMR spectra. In addition, slow motions of TM helices relative to one another may broaden resonance lines and thus further degrade spectral resolution. Nevertheless, we believe that these difficulties can be overcome and that it will be possible to solve structures of small helical bundle membrane proteins by solution NMR in the foreseeable future.

An interesting question is to what extent the micelle environment influences the NMR structures of membrane proteins. From the structures of OmpA and OmpX, which have been solved by NMR and crystallography, it is clear that the general features are independent of the structural method. Membrane proteins are also crystallized from micellar solutions, but crystal contacts could alter some structural details. In the case of OmpA, the extracellular loops are clearly much more mobile in the NMR than in the crystal structure (although *B*-factors are also increased in the loops). Perhaps related to the increased mobility of the loops, some β-strands are a little shorter in the NMR than in the crystal structure. However, the comparison is not completely straightforward because three loop residues were changed in crystallization trials in order to obtain a crystallizable protein [4]. These amino acid changes may have reduced the mobility of the loops and thereby may have promoted crystal formation. The situation in a more realistic membrane environment may be intermediate between the two extremes of crystallography and micellar solution NMR. Solid-state NMR of selectively labeled proteins may provide some answers to this question.

The ability to directly measure the dynamics of membrane proteins by NMR opens new windows to help understand the functions of this important class of proteins. We anticipate that measurements of dynamics will become one of the real benefits of NMR of membrane proteins. Other benefits that are not so easily realized by crystallography may include measurements of general and specific interactions with lipids [29]. Clearly, solution NMR has a lot to offer to further our understanding of the structure and function of membrane proteins!

Acknowledgements: This work was supported by NIH Grants GM51329 and AI30557 to L.K.T. F.A. and H.B. were supported by NIH Grant RR02301 to John Markley.

References

[1] Opella, S.J. (1997) Nat. Struct. Biol. NMR Suppl. 845–848.
[2] Pervushin, K., Riek, R., Wider, G. and Wüthrich, K. (1997) Proc. Natl. Acad. Sci. USA 94, 12366–12371.
[3] Sonntag, I., Scharc, H., Hirota, Y. and Henning, U. (1978) J. Bacteriol. 136, 280–285.
[4] Pautsch, A. and Schulz, G.E. (1998) Nat. Struct. Biol. 5, 1013–1017.
[5] Arora, A., Abildgaard, F., Bushweller, J.H. and Tamm, L.K. (2001) Nat. Struct. Biol. 8, 334–338.
[6] Vogel, H. and Jähnig, F. (1986) J. Mol. Biol. 190, 191–199.
[7] Kleinschmidt, J.H., den Blaauwen, T., Driessen, A.J.M. and Tamm, L.K. (1999) Biochemistry 38, 5005–5016.
[8] Saint, N., El Hamel, C., De, E. and Mollé, G. (2000) FEMS Microbiol. Lett. 190, 261–265.
[9] Arora, A., Rinehart, D., Szabo, G. and Tamm, L.K. (2000) J. Biol. Chem. 275, 1594–1600.
[10] Ried, G. and Henning, U. (1987) FEBS Lett. 223, 387–390.
[11] Van Alphen, L., Havekes, L. and Lutgenberg, B. (1977) FEBS Lett. 75, 285–290.
[12] Morona, R., Krämer, C. and Henning, U. (1985) J. Bacteriol. 164, 539–543.
[13] Chai, T. and Foulds, J. (1974) J. Mol. Biol. 85, 465–474.
[14] Dornmair, K., Kiefer, H. and Jähnig, F. (1990) J. Biol. Chem. 265, 18907–18911.
[15] Kleinschmidt, J.H., Wiener, M. and Tamm, L.K. (1999) Protein Sci. 8, 2065–2071.
[16] Surrey, T. and Jähnig, F. (1992) Proc. Natl. Acad. Sci. USA 89, 7457–7461.
[17] Kleinschmidt, J.H. and Tamm, L.K. (1996) Biochemistry 35, 12993–13000.
[18] Lipari, G. and Szabo, A. (1982) J. Am. Chem. Soc. 104, 4546–4559.
[19] Lipari, G. and Szabo, A. (1982) J. Am. Chem. Soc. 104, 4559–4570.
[20] Tjandra, N., Feller, S.E., Pastor, R.W. and Bax, A. (1990) J. Am. Chem. Soc. 117, 12562–12566.
[21] Bond, P.J., Feraldo-Gomez, J.D. and Sansom, M.S.P. (2002) Biophys. J. 83, 763–775.
[22] Han, X., Bushweller, J.H., Cafiso, D.S. and Tamm, L.K. (2001) Nat. Struct. Biol. 8, 715–720.
[23] Altenbach, C., Greenhalgh, D.A., Khorana, H.G. and Hubbell, W.L. (1994) Proc. Natl. Acad. Sci. USA 91, 1667–1671.
[24] Qiao, H., Armstrong, R.T., Melikyan, G.B., Cohen, F.S. and White, J.M. (1999) Mol. Biol. Cell 10, 2759–2769.
[25] Li, Y., Han, X. and Tamm, L.K. (2003) Biochemistry 42, 7245–7251.
[26] Tamm, L.K. (2003) Biochim. Biophys. Acta 1614, 14–23.
[27] Fernández, C., Adeishvili, K. and Wüthrich, K. (2001) Proc. Natl. Acad. Sci. USA 98, 2358–2363.
[28] Hwang, P.M., Choy, W.Y., Lo, E.I., Chen, L., Forman-Kay, J.D., Raetz, C.R.H., Privé, G.G., Bishop, R.E. and Kay, L.E. (2002) Proc. Natl. Acad. Sci. USA 99, 13560–13565.
[29] Fernández, C., Hilty, C., Wider, G. and Wüthrich, K. (2002) Proc. Natl. Acad. Sci. USA 99, 13533–13537.